Swansea University
Prifysgol Abertawe

Cronfa
Setting Research Free

Cronfa - Swansea University Open Access Repository

This is an author produced version of a paper published in :
Journal of Physics: Condensed Matter

Cronfa URL for this paper:
http://cronfa.swan.ac.uk/Record/cronfa30247

Structure and magnetic property of potassium intercalated pentacene: observation of superconducting phase in

KxC22H14

Takeshi Nakagawa1,5, Zhen Yuan1, Jun Zhang1, Kirill V Yusenko2, Christina Drathen3, QingQing Liu1, Serena Margadonna2   and Changqing Jin1,4

[1] Beijing National Laboratory for Condensed Matter Physics, Institute of Physics, Chinese Academy of Sciences, Beijing 100190, People's Republic of China

. [2] College of Engineering, Swansea University, Swansea, SA2 8PP, UK

. [3] ESRF, 71 Avenue Des Martyrs, F-38043 Grenoble cedex, France

. [4] Collaborative Innovation Centre of Quantum Matter, Beijing 100190, People's Republic of China

E-mail: jin@iphy.ac.cn

Abstract

We report the results from systematic investigations on the structure and magnetic properties of potassium intercalated pentacene as a function of potassium content, KxC22H14 ($1 \leqslant x \leqslant 3$). Synchrotron radiation powder x-ray diffraction technique revealed that there are two   different stable phases can be obtained via potassium intercalation, namely, K1C22H14 phase and K3C22H14 phase. Structural phase transition was induced when the potassium content

was increased to the nominal value $x = 3$. This phase transition is accompanied by drastic change in their magnetic property, where those samples with compositions K1C22H14 shows ferromagnetic behavior and those with near K3C22H14 lead to observation of superconductivity with transition temperature, $Tc,$ of 4.5 K. It is first time that superconductivity was observed in linear oligoacenes. Both magnetization study and synchrotron radiation powder x-ray diffraction clearly indicates that the superconducting phase belong to K3C22H14 as a result of phase transition from triclinic to monoclinic structure induced by chemical doping.

Introduction
Search for the superconductivity in organic compounds started in early 1960s and the first organic superconductor was dis- covered by intercalating electron acceptor to (TMTSF)2X and *β-(BEDT-TTF)2X* organic compounds [1]. The discovery of the conducting organic compounds has attracted considerable interest as they showed phenomenon that was not observed in other conventional superconductors. Recently, in 2010, Mituhashi and co-workers reported that a new carbon-based superconductor was discovered which has generated quite some excitement and renewed the importance of organic molecular solids once again [2]. Significance of this discovery can be denoted by the observation of superconductivity in a polycy- clic aromatic hydrocarbon (PAH) based material for the first

(a)
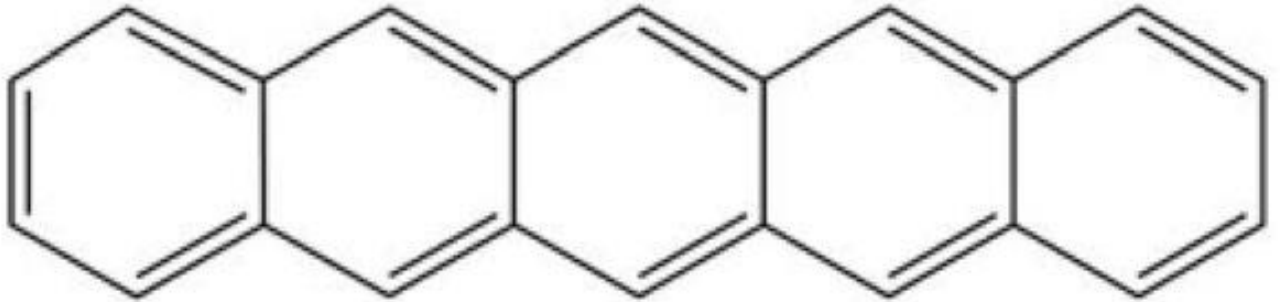
(c)
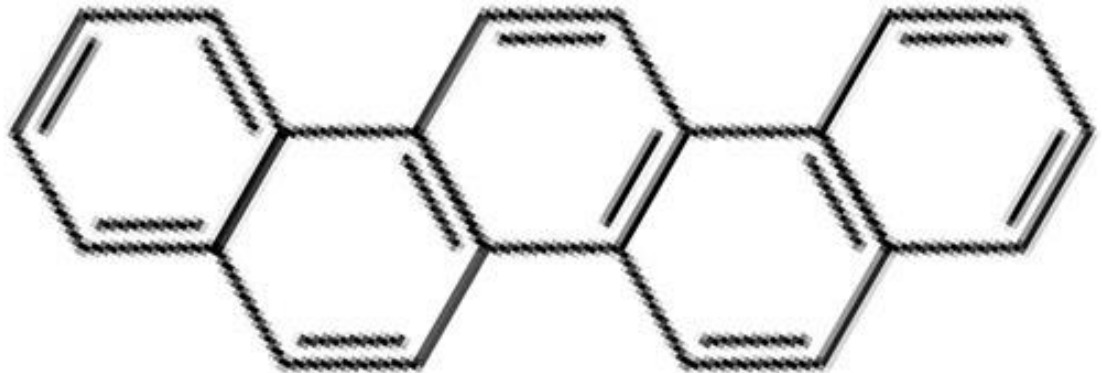
Figure 1. (a) Molecular structure of pentacene. (b) Crystal structure of pentacene viewed from *a-direction.* (c) Molecular structure of picene.

time, where the organic component contains only carbon and hydrogen atoms. The superconducting transition is observed with critical temperature, *Tc* up to 18K

when potassium inter- calatesintothecrystallatticeofpicene(C22H14),ofwhichfive benzene rings fused in zig-zag conformation. Soon after, super- conductivity in other PAH based materials has been reported on alkali-metal intercalated phenanthrene (C14H10), chrysene (C18H12), coronene (C24H12), and dibenzopentacene (C30H18) with Tc ranging from 5 to 33K [3–6]. The observed Tc values of 33 K is comparable to that observed in the most well-known family of carbon based superconductors, the alkali-metal doped fullerides (A3C60), which display Tc as high as 38K under application of pressure [7]. The high values of Tc in A3C60 has been understood by applying the conventional Bardeen– Cooper Schrieffer (BCS) theory until recently, but these systems have also emerged as archetypal examples of strongly correlated electron systems [8]. Similar to the cuprates high-Tc supercon- ductors, the superconductivity in Cs3C60 originates from an antiferromagnetic Mott insulator state highlighting again the importance of magnetic correlations for the paring mechanism.

PAH based molecular solids have been attracting a consid- erable amount of interest for their high degree of electronic delocalization where their properties can be easily modified by doping with electron acceptors or donors. This results in drastic changes in carrier mobility with different systems exhibiting metallic, insulating, semiconducting, and superconducting behavior[9,10].Thediscoveryofthisnewclassoforganic,low dimensional, high-Tc π-$electron$ superconductors is expected to open new possibilities in superconductivity research. However, mostly due to the difficulties in the synthesis of single phase materials, the exact characterization of their properties, chem- ical composition, crystal and electronic structure has proven to be challenging and many questions regarding the occurrence and mechanism of superconductivity remains unanswered [11]. An overview of both achievements and unsolved problems in PAH based superconductivity are discussed in [4].

In this report, we present results from the synthesis and characterization of potassium intercalated pentacene (KxC22H14) with various doping level to understand how their physical properties being affected by increasing elec- tron doping. Pentacene has same number of the benzene rings

with picene, which are fused linearly to form the molecule, while the picene has zig-zag conformation (figure 1). Their molecular structures are characterized by weak van der Waals interaction between the individual molecules. Picene and Pentacene are often compared as an example to emphasize that the physical properties of PAH are strongly affected by their molecular structure especially when the mechanism for the occurrence of superconductivity was discussed. Indeed, up until now, superconductivity was only observed with those PAHs in zig-zag conformation, but none were reported for linearly arranged ones. Recent elastic and inelastic electron scattering studies on metal-doped pentacene thin

films have showed that the successful charge transfer from alkali-metal to the pentacene induces the changes in the electronic struc- ture [12]. Conductivity of the thin films was controlled by the number of electrons donated from alkali-metals to the lowest unoccupied molecular orbitals (LUMO) of the pentacene and reported a Mott metal–insulator transition driven by electron– electron interaction [13, 14]. Significant increase in the con- ductivity was also observed for the hole doping to the highest occupied molecular orbitals (HOMO) of the pentacene [15]. The magnetic susceptibility measurement on the potassium doped pentacene in earlier report showed the presence of anti- ferromagnetic-like behavior, making K-pentacene a possible antiferromagnetic Mott insulator with strong electronic cor- relation similar to the case of intercalated C60 [7]. However, our recent magnetization measurements on K3Pentacene (K3C22H14) clearly showed that this material undergoes a superconducting phase transition at 4.5K, making it the first example of a superconductor based on the non-zig-zag, linear oligoacene. Here, we present the results obtained from sys- tematic investigations on newly prepared potassium inter- calated pentacene compounds with two different potassium doping level in order to understand how their physical proper- ties changes with increasing electron doping.

Experimental method

Polycrystalline samples with nominal composition $K_xC_{22}H_{14}$ (x = 1 and 3) were prepared by reacting stoichiometric amount

2

$\lambda = 1.5405$ Å
Space group: P-1
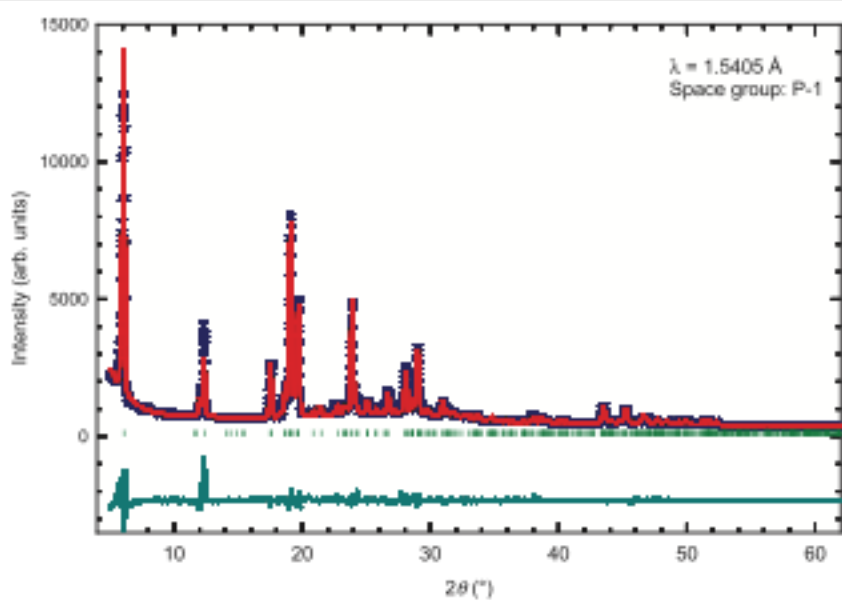
Figure 2. Observed (cross) and calculated (solid line) XRD pattern for pentacene phase H (C22H14) obtained using Cu Kα x-ray source. The lower solid line shows the difference between observed and calculated profiles and the tick marks show the reflection positions.

of pristine pentacene (purified by sublimation, TCI Chemicals) and potassium (K, >99.95%, Alfa Acer). Both potassium and pentacene were loaded into a small quartz container without mixing and placed separately so that they will not have direct contact. They were then loaded into longer quartz tube, sealed under vacuum, and annealed at 523K for 35h. The cooling process after annealing was varied for different batches of samples, namely, K1C22H14 and K3C22H14_A were quenched into liquid nitrogen, K3C22H14_B employed ramp rate of 3 K min−1, and K3C22H14_C employed 1 K h−1. As the starting materials and resulting compounds are both extremely sen- sitive to air/moisture, the whole procedures were carried out inside a glovebox filled with Ar where the oxygen and moisture levels were kept to less than 1 ppm. Approximately 10 mg of the resulting powder was pressed into pellets with a diameter of 5 mm and then placed inside a high quality quartz tube, sealed under vacuum. This tube was then loaded into the standard magnetic property measurement system (MPMS) from quantum design for the magnetization measurements (20 Oe, ZFC/FC). In order to confirm the observed signal is not machine dependent, newly prepared pellet was covered by Silicon vacuum grease to avoid exposure to air and placed on a brass tube and loaded into the MPMS 3 (VSM, Quantum design) and carried out same magnetization measurements. Another few milligram of the powder were sealed in the thin- wall glass capillaries for the synchrotron powder x-ray dif- fraction performed on the BM1A Swiss Norwegian beam line at european synchrotron radiation facility (ESRF), Grenoble ($\lambda = 0.688\ 94$ Å) and for Raman spectroscopy measurements using a krypton laser tuned at 783 nm [16].

Results

The powder x-ray diffraction (XRD) profile of as purchased pentacene powder shows the two already known polymorphs of pentacene **C** (low density phase) and **H** (high density

Table 1. Lattice parameters of two different polymorphs of pentacene, namely phase C and H.

a (Å) *b* (Å) *c* (Å) *α* (°) *β* (°) *γ* (°) *V* (Å3)

d(001) (Å) *θ* (°)

Phase C24

7.90

6.06 16.01

101.9 112.6 85.8

692.38 14.50 140.14

Phase H25

6.266

7.775 14.53 76.475 87.68 84.68

685.15 14.12 162.26

This work

6.259(1)

7.777(1) 14.538(2) 76.44(1) 87.64(1) 84.66(1) 687.9 (4)

14.05

—

phase) phases with weight fraction 3:7. Single phase **H** speci- mens, adopt triclinic structures, were obtained by sublima- tion at 573 K. The powder XRD profile of sublimed specimen is shown in figure 2 (Cu Kα λ = 1.54 Å). The refined lat- tice parameters *a, b,* and *c,* are 6.259(1) Å, 7.777(1) Å, and 14.538(2) Å, the angles α, β, and γ are 76.44(1)°, 87.64(1)°, and 84.66(1)°, respectively. The obtained values are compa- rable to those already reported for phase **H** (table 1) [17].

Compared to polymorph **C,** polymorph **H** has interchanged *a* and *b* axes, a smaller *d-spacing,* and different α and β angles. Furthermore, the herringbone angle, which is defined as the angle between the normal vectors to the molecular planes of the two inequivalent molecules, increases approximately by 20° [18, 19].

Upon potassium doping, it is expected that the alkali- metal ions will enter the lattice by expanding the spacing between the pentacene molecules resulting in a structure distortion, which in turn modifies their magnetic property. Indeed, while pristine pentacene does not show any mag- netism, the field dependent magnetization measurement at 2 K on K1Pentacene (K1C22H14) clearly shows ferromagnetic behavior (figure 3). The XRD pattern of K1C22H14 shows the

Figure 3. *M* versus *H* plot for K1C22H14 at 2 K measured between −5000 and 5000 Oe.

(0 0 *l)* Bragg peaks shifting towards lower 2θ angles, resulting in an increase of the *c-lattice* parameter from 14.538 (2) Å to 15.7330 (3) Å, while no structural change was observed. Obtained unit cell volume, *V,* of K1C22H14 also increases by intercalation of potassium metal, which contrasts with the K-picene case where the decrease in *V* was observed upon potassium doping [5].

Significant changes in both the XRD pattern and magneti- zation measurements were observed when the potassium con- centration was increased to the nominal value of $x = 3$. The appearance of new reflections and a substantial redistribution of the peaks intensity provide a clear indication of higher levels of doping induce a structural transition. The electron transfer from alkali-metal to organic molecule was also confirmed by comparing Raman spectroscopy of pristine pentacene and K3C22H14 (see supplementary figure S1 (stacks.iop.org/ JPhysCM/28/484001/mmedia)). Figure 4 shows the temper- ature and magnetic field dependence of the dc magnetization of a typical K3C22H14 in pellet form sample measured in both zero-field cooled (ZFC) and field-cooled (FC) conditions. The sample was first cooled down to 2 K under zero-field cooling, and then a magnetic field of 20 Oe was applied. The onset of a well-defined superconducting transition was observed at 4.5 K and this was followed by magnetic field dependent measure- ment at 2 K. Observed *M-H* curve clearly indicates the differ- ence from that of K1C22H14, showing typical superconducting behavior.

We have attempted to get further insights into the crystal structure of this newly formed phase. A best auto-indexed lat- tice was obtained on peak-fitted locations after the exclusion of a minor pentacene component. The lattice parameter was optim- ized using a Le Bail fit in GSAS [20]. The observed indexed intensities were then manually matched by manipulating two rigid and independent pentacene molecules for translation and rotation and tilt within this lattice (in P1) for an approximate trial solution. Once completed, the symmetry search for the

model was carried out using Endeavour [21]. Symmetry of P21/c was automatically applied and the lattice morphology adjusted appropriately. K atoms were introduced by cycling difference Fourier maps based on this fixed model. The final tentative model structure was then rigid-body refined, and the resulting lattice constants are $a = 15.718(4)$ Å, $b = 10.279(5)$ Å, $c = 4.170(3)$ Å and $\beta = 99.6°$, $V = 671.6$ (3) Å3 (figure 5).

Through our exploration of other possible model-building choices, we can

highlight some parallels and contrasts with other proposed structural options. For example, the loss of the herringbone arrangement of pentacene molecules to π-*stacking* in the proposition of Hansson *et al* is not evident in our model, which remains herringbone—at a reduced intermolecular angle of ~85° and with K sites located at intermolecular posi- tions [22]. All our attempts to produce the structural models following the descriptions of the result of DFT calculations lead to significant deviations from the observed intensities. Nonetheless, stacking aside, the potassium positions shown here are comparable to the near-terminal (intralayer) and mid- moleclular (interlayer) positions described by Hansson *et al's* in their *a* and *b* phase models [22]. It is relevant to notice that the results of our preliminary analysis indicate that the lattice volume of the phase with nominal composition K3C22H14 is smaller than that of the pristine material (listed in table 2). Such volume contraction upon metal intercalation has been reported previously for similar systems and it has been justi- fied in terms of distortions of the herringbone structure and intralayer positioning (as opposed to interlayer) of the K [3]. Direct comparison between our model and pentacene- H shows evidence of both shortened terminal H–H contact distances between molecules and increased layer separation but no significant departure from the herringbone structure (figure 6). Further detailed structural studies are necessary to clarify this point.

It should be noted here that the magnetization measure- ments were repeated several times using both MPMS and

Figure 4. Temperature dependence of magnetization for K3Pentacene. (a) *M/H* versus *T* plot for pellet sample of K3Petancene with Tc = 4.5 K in ZFC/FC measurements with applied magnetic field of 20 Oe. Superconducting volume fraction was estimated to be 0.5%. Inset: *M* versus *H* plot for K3Pentacene at 2 K (selected region). The lower critical magnetic field, *Hc1,* was estimated to be ~180 Oe. (b) *M* versus *H* plot at 2 K (whole range).

MPMS 3 machines in order to confirm that observed trans- ition is not machine and/or measurement technique dependent. This superconducting transition was observed when K3C22H14 was obtained from intercalating potassium to polymorph **H** only pentacene but not observed when K3C22H14 was pre- pared using polymorph **C** only pentacene (see supplementary figure S2). Furthermore, it was found that independent of the synthetic conditions, where good samples always show exactly the same transition temperature of 4.5 K, while the supercon- ducting volume fraction and critical magnetic field varied between different batches. This implies that, unlike K-Picene case, only one superconducting phase should exist upon elec- tron doping of pentacene. On the other hand, the different cooling rates from 523 K down to room temperature seem to have a significant effect on the formation of different phases. This was apparent when the magnetization of each sample was measured as a function of applied magnetic

field at 2 K. In particular, when the sample was quenched in liquid nitrogen

from 523 K (sample A) or when a rate of 3 K min−1 was used to reach room temperature (sample B), they showed mixed ferromagnetic and superconducting behavior. While when the sample was cooled at the rate of 1 K h−1, the M versus H curves clearly show a superconducting behavior (sample C). The temperature dependent dc magnetization measurements of these samples are shown in the supplementary information (see supplementary figure S3). The corresponding synchro- tron XRD measurements show that fast cooling tends to yield a mixture of K1- and K3C22H14 phases, while slow cooling predominantly leads to the formation of only K3C22H14.

The superconducting shielding fraction was estimated to be 0.5% from the magnitude of the ZFC curve (estimated den- sity 1.86 g cm−3). Although, the observed drop in the magnet- ization measurement is clear and sharp, the superconducting shielding fraction is extremely small, which seems to be a common feature for most PAH based superconductors. For instance, in K-doped picene, the obtained shielding fraction

Figure 5. Observed (cross) and calculated (solid line) XRD pattern for K3C22H14

obtained at BM1A (ESRF, $\lambda = 0.688\ 94$ Å). The lower solid line shows the difference between observed and calculated profiles and the tick marks show the reflection positions.

was 1.2% [2]. These small fractions observed are possibly caused by a nano-sized particle effects that would consider- ably reduce the bulk volume fraction due to larger ratio of surface over bulk. Other possibilities could be a non-optimal doping level, in some cases it has been possible to increase the fraction by varying the nominal composition slightly, or inhomogeneity of the end product [23]. The lower critical magnetic field, $Hc1$, and upper critical magnetic field, $Hc2$ were estimated to be ~180 Oe and 7000 Oe from the M versus H plot at 2K (figure 4 inset), respectively. The Ginzburg– Landau coherence length (ξGL) was evaluated, using general equation relating $Hc2$ and ξGL, to be 18.4nm [24], which is comparable to those values reported for K3Phenanthrene (18 nm) [25].

Discussion

The key factor to understand the mechanism of supercon- ductivity in metal doped PAH systems is thought to be the existence of low-lying, unoccupied *π-electronic* states, which accept electrons from the dopants. In the case of picene, the conduction bands comprise from four bands with significantly narrow width, derived from LUMO and LUMO+1, which have almost the same energy. The superconducting phase appears when the picene molecules accept three electrons from the alkali-metal (A3Picene, A = K and Rb), that is when the LUMO is fully

occupied and LUMO+1 is half occupied. When less/more electrons are accepted, Pauli/Curie type para- magnetic behavior is observed [5].

The existence of degenerate electron-accepting orbitals is somewhat similar to other families of π-*electron* based super- conductors, such as metal-doped graphite and C60 compounds. Naturally, high molecular symmetry gives rise to degenerate orbitals, for example triple degeneracy in the C60 buckyballs (point group *Ih),* or doubly-degenerate *e1g* LUMO's in coro- nene, a disk-like molecule, which consists of six benzene rings

Table 2. Lattice parameters for pentacene and K-doped pentacene.

| a (Å)	b (Å)	c (Å)	α (°)	β (°)	γ (°)	V (Å3)
Pentacene (H)						
6.259(1)	7.777(1)	14.538(2)	76.44(1)	87.64(1)	84.66(1)	687.9 (4)
K1Pentacene						
6.211 (3)	7.629 (3)	15.733 (9)	76.48 (6)	87.74 (5)	85.09 (3)	725.4 (4)
K3Pentacene						
15.718 (4)	10.279 (4)	4.170 (3)	90.0	99.62	90.0	671.6 (3)

fused together (point group *D6h)* [26, 27]. Electron-doped cor- onene (K3Coronene) was also reported to show signature of superconducting phase below 15 K [5].

However, in picene (point group *C2v)* the degeneracy does not arise from the symmetry, but rather from the extremely small band gap between LUMO and LUMO+1 forming the conduction band [28]. Along the same lines, although dibenzopentacene (point group *C2v)* has a large energy gap between the LUMO and the LUMO+1, the LUMO+1 and the LUMO+2 are nearly-degenerate [29].

The occurrence of this so called 'accidental' degeneracy has only been observed in those PAH that are fused rings in a zig-zag fashion.

In pristine pentacene, on the other hand, the symmetry is also too low (point group *D2h)* and the band gaps between LUMO and LUMO+1, and LUMO+1 and LUMO+2 is too large to derive both natural and accidental degeneracy (supplementary figure S4) [30]. This is because while in picene they are fused in a zig-zag conformation, in penta- cene they are arranged linearly. Recent band structure calcul- ations have shown that the electronic properties of these PAH materials are sensitively influenced by their molecular size, arrangements and orientations [31]. Significant differences in electronic band structure are observed for picene and pentacene despite they both consist of five benzene rings.
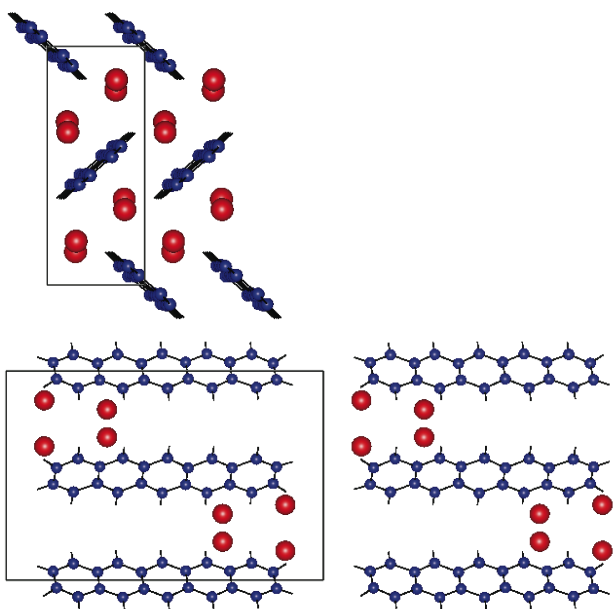
Figure 6. Proposed structure model of K3C22H14 viewed from (left) *a-direction* (right) *c-direction.* K-atom is indicated by red spheres and C-atom is indicated by blue spheres.

It was reported that the calculated band gap between LUMO and LUMO+1 for picene are significantly smaller (0.15 eV) than in pentacene molecule (1.28 eV) [4]. The occurrence of orbital degeneracy in pentacene must therefore be different in nature from those discussed above. Instead, the influence of the crystal structure transition on the electronic property of pristine PAH molecule has to be considered. We recall that pentacene possesses two polymorphs, namely phase **C** and **H.** Even though the difference in crystal structure between the two phases is rather small, significant changes in the band structure are observed. In particular, the band dispersions are enhanced in phase **H,** that is, both valence and conduction band are widened in the herringbone plane [32]. While doping alkali-metals in low concentrations results in an increase of intermolecular distances of penta- cene, no structural phase transition was observed [33, 34]. The structural transition from triclinic to monoclinic struc- ture, reported in this work, was induced by a further increase of the metal concentration. This drastic modification in a crystal lattice to

a higher symmetry will definitely lead to a change in electronic band structure, potentially giving rise to orbital degeneracy. This in turn, would permit orbitals to accept electrons from the alkali-metals into the conduction band and to generate the high carrier density required for superconductivity.

Conclusion

The discovery of superconductivity in potassium doped pen- tacene could stimulate the investigation of other linear oli- goacenes. One of the characteristic properties of the linear oligoacenes is that the energy gap between HOMO and LUMO is known to decrease as more benzene rings are added; anthracene, 4.1eV; tetracene, 3.1eV, and pentacene, 2.5eV (n = 3, 4, and 5 rings, respectively) [32]. Particular attention should be put on how the superconducting transition temper- ature varies with the number of benzene rings.

To summarize, we have successfully synthesized potas- sium intercalated pentacene with different electron doping levels. The electron doping was confirmed by Raman scat- tering. For a small doping level, $K_1C_{22}H_{14}$, ferromagnetic behavior was clearly observed, but no superconducting trans- ition. When doping level is increased, namely in $K_3C_{22}H_{14}$, a

superconducting transition is observed at 4.5 K. Furthermore, increasing the doping level in K-Pentacene induces a dramatic change from the triclinic cell adopted by pristine pentacene to a monoclinic structure. This is the first time that the supercon- ductivity was observed in a PAH material in which benzene rings are fused in line.

Acknowledgment

Author contributions

TN have prepared all the samples mentioned in this paper, carried out laboratory experiments, analyzed obtained data with helps of the collaborators, and wrote the manuscript. ZY carried out Raman spectroscopy measurement, JZ has helped prepare samples, CD and KVY have carried out synchrotron XRD measurements. QQL has helped analysis of exper- imental data. SM have carried out structure analysis and pro- vided important comments and discussion in whole process. CJ was responsible for the overall project. All Authors partici- pated in discussion of the manuscript.

Competing financial interest

The authors declare no competing financial interests.

References

[1] Jerome D 2004 Organic conductors: from charge density wave TTF-TCNQ to superconducting (TMTSF)2PF6 *Chem. Rev.* **104** 5565–91

[2] Mitsuhashi R *et al* 2010 Superconductivity in alkali- metal-doped picene *Nature* **464** 76

[3] Wang X F *et al* 2011 Superconductivity at 5 K in alkali- metal-doped phenanthrene *Nat. Commun.* **2** 507

[4] Artioli G *et al* 2015 Superconductivity in Sm-doped [n] phenacenes (n = 3, 4, 5) *Chem. Commun.* **51** 1092–5

[5] Kubozono Y *et al* 2011 Metal-intercalated aromatic hydrocarbons: a new class of carbon-based superconductors *Phys. Chem. Chem. Phys.* **13** 16476

[6] Xue M *et al* 2012 Superconductivity above 30 K in alkali- metal doped hydrocarbon *Sci. Rep.* **2** 389

[7] Ganin A Y *et al* 2008 Bulk superconductivity at 38 K in a molecular system *Nat. Mater.* **7** 367

[8] Takabayashi Y *et al* 2009 The disorder-free non-BCS superconductor Cs3C60 emerges from an antiferromagnetic insulator parent state *Science* **323** 1585

[9] Saito G and Yoshida Y 2007 Development of conductive organic molecular assemblies: organic metals, superconductors, and exotic functional materials *Bull. Chem. Soc. Japan* **80** 1

[10] Fang B, Zhou H and Honma I 2005 Electrochemical lithium doping of a pentacene molecule semiconductor *Appl. Phys. Lett.* **86** 261909

[11] Heguri S, Kobayashi M and Tanigaki K 2015 Questioning the existence of superconducting potassium doped phases for aromatic hydrocarbons *Phys. Rev.* B **92** 014502

[12] Roth F *et al* 2015 Impact of potassium doping on the electronic structure of tetracene and pentacene: an electron energy-loss study *J. Chem. Phys.* **143** 154708

[13] Craciun M F, Giovannetti G, Rogge S, Brocks G, Morpurgo A F and van den Brink J 2009 Evidence for the formation of a Mott state in potassium-intercalated pentacene *Phys. Rev.* B **79** 125116

[14] Minakata T, Ozaki M and Imai H 1993 Conducting thin-film of pentacene doped with alkaline-metals *J. Appl. Phys.* **74** 1079

[15] Minakata T, Nagoya I and Ozaki M 1991 Highly ordered and conducting thin-film of pentacene doped with iodine vapor *J. Appl. Phys.* **69** 7354

[16] Mori T and Ikehata S 1997 Low temperature magnetic properties of potassium doped pentacene *J. Appl. Phys.* **82** 5670–3

[17] Alajtal A I, Edwards H G M, Elbagerma M A and Scowen I J 2010 The effect of laser wavelength on the Raman Spectra of phenanthrene, chrysene, and tetracene: implications for extra-terrestrial detection of polyaromatic hydrocarbons *Spectrochim. Acta* A **76** 1

[18] Mattheus C C, Dros A B, Baas J, Meetsma A, de Boer J L and Palstra T T M 2001 Polymorphism in pentacene *Acta Cryst.* C **57** 939

[19] Campbell R B, Trotter J and Robertson J M 1961 Crystal and molecular structure of pentacene *Acta Cryst.* **14** 705

[20] Larson A C and Von Dreele R B 1994 GSAS-general structure analysis system *Los Alamos National Laboratory Report* LAUR 86-748 University of California

[21] Putz H, Shoen J C and Jansen M 1999 Combined method for ʹab *initio'* structure solution from powder diffraction data *J. Appl. Cryst.* **32** 864–70

[22] Hansson A, Böhlin J and Stafström S 2006 Structural and electronic transitions in potassium-doped pentacene *Phys. Rev.* B **73** 184114

[23] Holczer K *et al* 1991 Alkali-fulleride superconductors— synthesis, composition and diamagnetic shielding *Science* **252** 1154

[24] Tinkham M 1975 *Introduction to Superconductvity* (New York: McGraw-Hill)

[25] Kubozono Y 2015 Superconductivity in aromatic hydrocarbons *Physica* C **514** 99–205

[26] Echigo T, Kimata M and Maruoka T 2007 Crystal-chemical and carbon-isotopic characteristics of karpatite (C24H12) from the Picacho Peak Area, San Benito County, California: evidences for the hydrothermal formation *Am. Mineral.*

92 1262   [27] Kosugi T, Miyake T, Ishibashi S, Arita R and Aoki H

2011 *Ab initio* electronic structure of solid coronene: differences from and commonalities to picene *Phys. Rev.* B **84** 020507

[28] Kosugi T, Miyake T, Ishibashi S, Arita R and Aoki H 2011 First-principles structural optimization and electronic structure of the superconductor picene for various

potassium doping levels *Phys. Rev.* B **84** 214506

[29] Mahns B, Friedrich R, Konig A, Grobosch M, Knupfer M and Hahn T 2012 Electronic properties of 1,2;8,9-dibenzopentacene thin films: a joint experimental and theoretical study *Phys. Rev.* B **86** 035209

[30] Kim M, Choi H C, Shim J H and Min B I 2013 Correlated electronic structures and the phase diagram of hydrocarbon- based superconductors *New J. Phys.* **15** 113030

[31] Kato T and Yamabe T 2006 Vibronic intercations in the positively charged p-conjugated hydrocarbons *Chem. Phys.* **325** 437–44

[32] Hummer K and Ambrosh-Draxl C 2005 Electronic properties of oligoacenes from first principles *Phys. Rev.* B **72** 205205

[33] Matsuo Y, Sasaki S and Ikehata S 2004 Stage structure and electrical properties of rubidium-doped pentacene *Phys. Lett.* A **321** 62–6

[34] Matsuo Y, Suzuki T, Yokoi Y and Ikehata S 2004 Stage structure in cesium doped pentacene *J. Phys. Chem. Solids* **65** 619–21